

Kinetic Investigation of the Inhibitory Effect of Gemcitabine on DNA Polymerization Catalyzed by Human Mitochondrial DNA Polymerase^{*[5]}

Received for publication, January 11, 2008, and in revised form, March 10, 2008. Published, JBC Papers in Press, March 31, 2008, DOI 10.1074/jbc.M800310200

Jason D. Fowler^{†§1}, Jessica A. Brown^{‡§2}, Kenneth A. Johnson[¶], and Zucui Suo^{‡§||*##3}

From the [†]Department of Biochemistry, the [‡]Ohio State Biochemistry Program, the [¶]Ohio State Biophysics Program, the ^{**}Molecular, Cellular and Developmental Biology Program, the ^{##}Comprehensive Cancer Center, The Ohio State University, Columbus, Ohio 43210 and the [¶]Institute for Cell and Molecular Biology, Department of Chemistry and Biochemistry, University of Texas, Austin, Texas 78712

Gemcitabine, 2'-deoxy-2',2'-difluorocytidine (dFdC), is a drug approved for use against various solid tumors. Clinically, this moderately toxic nucleoside analog causes peripheral neuropathy, hematological dysfunction, and pulmonary toxicity in cancer patients. Although these side effects closely mimic symptoms of mitochondrial dysfunction, there is no direct evidence to show gemcitabine interferes with mitochondrial DNA replication catalyzed by human DNA polymerase γ . Here we employed pre-steady state kinetic methods to directly investigate the incorporation of the 5'-triphosphorylated form of gemcitabine (dFdCTP), the excision of the incorporated monophosphorylated form (dFdCMP), and the bypass of template base dFdC catalyzed by human DNA polymerase γ . Opposite template base dG, dFdCTP was incorporated with a 432-fold lower efficiency than dCTP. Although dFdC is not a chain terminator, the incorporated dFdCMP decreased the incorporation efficiency of the next 2 correct nucleotides by 214- and 7-fold, respectively. Moreover, the primer 3'-dFdCMP was excised with a 50-fold slower rate than the matched 3'-dCMP. When dFdC was encountered as a template base, DNA polymerase γ paused at the lesion and one downstream position but eventually elongated the primer to full-length product. These pauses were because of a 1,000-fold decrease in nucleotide incorporation efficiency. Interestingly, the polymerase fidelity at these pause sites decreased by 2 orders of magnitude. Thus, our pre-steady state kinetic studies provide direct evidence demonstrating the inhibitory effect of gemcitabine on the activity of human mitochondrial DNA polymerase.

Many nucleoside analogs are potent anti-cancer and anti-viral drug compounds. Among 15 Food and Drug Administra-

tion-approved nucleoside analogs, gemcitabine or 2'-deoxy-2',2'-difluorocytidine (dFdC,⁴ supplemental Fig. 1) is an anti-cancer drug that is clinically used for the treatment of non-small cell lung cancer (1), pancreatic cancer (2), metastatic breast cancer (3), and ovarian cancer (4). It has also shown promising efficacy for the treatment of other solid tumors and hematological malignancies (5–12) suggesting more widespread use in the future. In addition to its use as a monotherapy, gemcitabine is often most effective when used as part of a combination therapy, frequently with platinum-based and topoisomerase-targeted chemotherapeutic agents (13–15).

Gemcitabine is administered in the form of a biologically inactive prodrug that first permeates the cellular membrane by facilitated diffusion (16, 17) almost exclusively via the human equilibrative nucleoside transporter number 1 (17, 18). Following transport, dFdC is metabolized to the biologically active monophosphorylated form (dFdCMP) by deoxycytidine kinase, which is the rate-limiting step during the activation of gemcitabine (19). Subsequently, dFdCMP is further phosphorylated to form the cytotoxic metabolites gemcitabine diphosphate (dFdCDP) and gemcitabine triphosphate (dFdCTP) by cellular kinases. It has been shown that dFdCTP competes effectively against endogenous dCTP for incorporation into genomic DNA (20) and against CTP into RNA (21), and that the proof-reading exonuclease activity of human DNA polymerase ϵ is essentially unable to remove dFdCMP once incorporated into DNA (22). Interestingly, dFdCTP incorporation by human DNA polymerase α results in "masked termination" of DNA synthesis where, following a single dFdCTP incorporation into DNA, the primer is extended by only one additional dNTP before polymerization is inhibited (20, 22). However, in addition to being incorporated into DNA and RNA, dFdCDP and dFdCTP are known to inhibit ribonucleotide reductase, thereby significantly decreasing cellular dCTP concentrations and leading to increased phosphorylation of dFdCDP (23, 24). Furthermore, high concentrations of dFdCTP inhibit CTP synthetase, whereby dCTP and CTP pools are further decreased

* This work was supported, in whole or in part, by National Institutes of Health Grants GM079403 (to Z. S.) and GM044613 (to K. A. J.). The costs of publication of this article were defrayed in part by the payment of page charges. This article must therefore be hereby marked "advertisement" in accordance with 18 U.S.C. Section 1734 solely to indicate this fact.

[5] The on-line version of this article (available at <http://www.jbc.org>) contains supplemental Figs. 1–3.

¹ Supported by American Heart Association Predoctoral Fellowship Grant GRT00004622.

² Supported by National Institutes of Health Chemistry and Biology Interface Program at The Ohio State University (Grant 5 T32 GM008512-11).

³ To whom correspondence should be addressed: 740 Biological Sciences, 484 West 12th Ave., Columbus, OH 43210. Tel.: 614-688-3706; Fax: 614-292-6773; E-mail: suo.3@osu.edu.

⁴ The abbreviations used are: dFdC, 2'-deoxy-2',2'-difluorocytidine; dFdCMP, gemcitabine 5'-monophosphate; dFdCDP, gemcitabine 5'-diphosphate; dFdCTP, gemcitabine 5'-triphosphate; FIAU, 1-(2-deoxy-2-fluoro- β -D-arabinofuranosyl)-5-iodouracil; pol γ , human DNA polymerase γ holoenzyme; mtDNA, mitochondrial DNA; SSU, human mtDNA polymerase small subunit.

Gemcitabine Inhibits Human DNA Polymerase γ

(25, 26). Reduced competition from diminished dCTP pools makes dFdCTP incorporation into DNA and RNA more probable, thus promoting cell cycle arrest and apoptosis and inhibiting DNA repair (23). Furthermore, dFdCMP and dFdCTP also inhibit dCMP deaminase, the major pathway by which dFdCMP is metabolized (27). The combined synergistic effect of these inhibitory activities is termed "self-potentialiation" and is illustrated in supplemental Fig. 2 (28, 29).

Moderate toxicity of gemcitabine has been observed in cancer patients with peripheral neuropathy (30, 31) and hematological dysfunction in which myelosuppression frequently emerges as the dose-limiting factor (4). The toxicological profile of gemcitabine resembles that of many other anti-viral nucleoside analogs and frequently mimics the symptoms of heritable mitochondrial defects (32). Furthermore, the unique susceptibility of the mitochondria to the toxic effects of nucleoside analog drugs makes it a prime suspect as the cause of gemcitabine-induced toxicity. An excellent precedent to support this hypothesis is the case of a related nucleoside analog drug developed by Lilly in the early 1990s. Fialuridine (FIAU), a nucleoside analog drug similar to gemcitabine but targeted toward hepatitis B, killed five patients in clinical trials (33, 34) due to the fact that FIAU is an excellent substrate for human mitochondrial DNA polymerase holoenzyme (pol γ) (33). Previously, we have used pre-steady state kinetic methods to evaluate the mitochondrial toxicity of several anti-HIV nucleoside analogs and the anti-hepatitis B nucleoside analog FIAU with recombinant pol γ (35). Our *in vitro* kinetic data correlate well with the observed toxicities of these drugs *in vivo* (36). Therefore, to evaluate the potential mitochondrial toxicity of gemcitabine, we again employed pre-steady state kinetic methods to evaluate the incorporation, extension, and excision of gemcitabine catalyzed by pol γ . In addition, we examined whether or not an incorporated gemcitabine as a template base might lead to mutations in the next round of mitochondrial DNA synthesis. Our resulting data provide direct evidence for the inhibitory effect of gemcitabine on the activity of human pol γ .

EXPERIMENTAL PROCEDURES

Materials—What follows is a list of the reagents used for these experiments and their sources: [γ - 32 P]ATP from GE Healthcare; Bio-Spin columns from Bio-Rad; dNTPs from Invitrogen; dFdCTP from Trilink Biotechnologies Inc. (San Diego); OptiKinase from U. S. Biochemical Corp.

Optimized Reaction Buffer G—Buffer G consisted of 50 mM Tris-Cl, pH 7.5, at 37 °C, 100 mM NaCl, and 2.5 mM MgCl₂. Note that all concentrations listed in this paper refer to the final concentration after mixing unless otherwise noted.

Optimized Reaction Buffer L—Buffer L consisted of 50 mM Tris-Cl, pH 8.4, at 37 °C, 100 mM NaCl, 5 mM MgCl₂, 0.1 mM EDTA, 5 mM dithiothreitol, 0.1 mg/ml bovine serum albumin, and 10% glycerol.

Optimized Reaction Buffer M—Buffer M consisted of 50 mM HEPES, pH 8.0, at 25 °C, 12 mM NaCl, 8.75 mM MgCl₂, 0.2 mM EDTA, 5 mM dithiothreitol, 0.1 mg/ml bovine serum albumin, and 10% glycerol.

Purification of Human Polymerase γ Subunits—Expression and purification of wild-type human DNA polymerase γ , its

exonuclease-deficient mutant E200A, and the small accessory subunit were carried out as described previously (35, 37).

Synthetic Oligodeoxyribonucleotides—All DNA substrates not containing gemcitabine were purchased from Integrated DNA Technologies (Coralville, IA) and purified by denaturing PAGE (17% acrylamide, 8 M urea). Concentrations of synthetic oligodeoxyribonucleotides were determined from their UV absorbance at 260 nm. Primers were 5'- 32 P-labeled by incubation with [γ - 32 P]ATP and OptiKinase at 37 °C for 1 h. The remaining [γ - 32 P]ATP was subsequently removed by size exclusion chromatography in a Bio-Spin 6 column. All primers were annealed to their respective templates in a 1:1.15 (primer: template) molar ratio by heating the mixture to 95 °C for 10 min and then slowly cooling to room temperature over ~6 h.

Synthetic Oligodeoxyribonucleotides Containing Gemcitabine—To create two DNA primers and a template that contain site-specific gemcitabine, a primer extension and ligation strategy was employed. Primer 23F-mer (Table 1) was synthesized by mixing DNA 22/41-mer (Table 1) with 5 μ M dFdCTP and human DNA polymerase μ (38), a template-directed DNA polymerase capable of efficiently incorporating dFdCTP, in reaction buffer M. The reaction was conducted for 2 h at 25 °C yielding maximum conversion of the 22-mer primer to 23F-mer (Table 1). A simultaneous control reaction was performed under identical conditions but substituting dCTP for dFdCTP. The products of both reactions were radiolabeled and compared using sequencing PAGE (17% acrylamide, 8 M urea) at single nucleotide resolution. The position of the 3'-dFdCMP-terminated 23F-mer was determined by comparison with the control reaction. The 23F-mer product was then gel-purified, thereby simultaneously removing any remaining unreacted 22-mer primer and any multiple incorporation products. A similar reaction and purification scheme was performed to synthesize primer 24FG-mer (Table 1) except 23F-mer was used as the starting primer.

To synthesize template 41F-mer (Table 1), the DNA substrate 21-19/35-mer (Table 1) was incubated with 8 μ M dFdCTP and human DNA polymerase λ (39), a template-directed, gap-filling DNA polymerase capable of efficiently incorporating dFdCTP, for 5 min at 37 °C in reaction buffer L to form the 21F-19/35-mer. Unreacted dFdCTP was then removed using gel filtration (Bio-Spin 6, Bio-Rad). The DNA solution was heated to 95 °C for 10 min and then slowly cooled to room temperature over 6 h to re-anneal 21F-19/35-mer (a nicked DNA substrate). A solution of 10 mM MgCl₂, 1 mM ATP, and T4 DNA ligase (11 units/ μ l) was added to the annealed DNA solution to ligate the nicked DNA for 7 min at 37 °C. The resulting 41F-mer was radiolabeled and compared with the control DNA template 41-mer (Table 1) using denaturing PAGE at single nucleotide resolution, thereby verifying both the incorporation of dFdCMP and the subsequent ligation of the primers. The resulting 41F-mer was then gel-purified to ensure homogeneity. Furthermore, the incorporation and position of the dFdCMP moiety into the 41F-mer template was additionally verified through observation of the pause pattern exhibited by pol γ as it encountered the dFdCMP moiety at the expected position in the template.

Single-turnover Nucleotide Incorporation Assay—All assays using pol γ were carried out at 37 °C in buffer G containing 2.5 mM MgCl₂. For single nucleotide incorporation assays, pol γ (90 nM) and its cofactor SSU (450 nM) were combined (1:5 molar ratio) and preincubated on ice in buffer G for 20 min to form human pol γ holoenzyme. Next, 30 nM of a DNA substrate containing a 5'-[³²P]-labeled DNA primer was added to the reconstituted holoenzyme (3:1 molar ratio, holoenzyme:DNA) and incubated on ice for an additional 20 min. The single nucleotide incorporation reaction was initiated by the addition of dNTP and 2.5 mM MgCl₂ in buffer G using a rapid chemical quench apparatus (KinTek, Clarence, PA). After varying reaction times at 37 °C, the reactions were quenched by the addition of 0.37 M EDTA.

Excision Reactions—For the 3' → 5'-exonuclease assay, wild-type pol γ (100 nM) and SSU (500 nM) in buffer G were first preincubated on ice for 20 min to form human pol γ holoenzyme and then mixed with 5'-³²P-labeled DNA substrate (75 nM) in the absence of Mg²⁺. The 3' → 5'-exonuclease reaction was initiated by the addition of 2.5 mM MgCl₂ in buffer G using a rapid chemical quench apparatus. After varying reaction times at 37 °C, the reactions were quenched by the addition of 0.37 M EDTA. The concentration of remaining full-length primer as a function of time was quantitated, and the exonuclease reaction time course (Fig. 2) was fit to Equation 3 or 4 to yield an excision rate constant.

Running Start Nucleotide Incorporation Assay—For the running start nucleotide incorporation assay, a DNA substrate (30 nM) was first preincubated with a solution of pol γ (90 nM) and SSU (450 nM) in buffer G as described above. This solution was rapidly mixed with MgCl₂ (2.5 mM) and dNTPs (100 μ M each). The primer elongation at various times was stopped by the addition of 0.37 M EDTA.

Product Analysis—Products of the polymerase and exonuclease reactions were separated by sequencing gel electrophoresis (17% acrylamide, 8 M urea, 1× TBE running buffer) and quantitated using a PhosphorImager 445 SI (GE Healthcare).

Data Analysis—Kinetic data were fit via nonlinear regression using KaleidaGraph (Synergy Software). Data from single-turnover nucleotide incorporation assays were fit to a single exponential (Equation 1) to obtain an observed incorporation rate constant (k_{obs}). The dNTP concentration dependence of k_{obs} was fit to a hyperbolic equation (Equation 2) to yield both the equilibrium dissociation constant (K_d) and the maximum nucleotide incorporation rate constant (k_p). Single-phase exonuclease reaction time courses were fit to a single exponential equation (Equation 3) to yield the exonuclease rate constant (k_{exo}). Biphasic exonuclease reaction time courses were fit to a double exponential (Equation 4) to yield $k_{\text{exo},1}$ and reaction amplitude A_1 in the fast phase and $k_{\text{exo},2}$ and reaction amplitude A_2 in the slow phase.

$$[\text{Product}] = A(1 - \exp(-k_{\text{obs}}t)) \quad (\text{Eq. 1})$$

$$k_{\text{obs}} = k_p[\text{dNTP}]/\{[\text{dNTP}] + K_d\} \quad (\text{Eq. 2})$$

$$[\text{Product}] = A(\exp(-k_{\text{exo}}t)) \quad (\text{Eq. 3})$$

$$[\text{Product}] = A_1(\exp(-k_{\text{exo},1}t)) + A_2(\exp(-k_{\text{exo},2}t)) \quad (\text{Eq. 4})$$

RESULTS

Determination of the Pre-steady State Kinetic Parameters for dFdCTP and dCTP Incorporation—The kinetic mechanism of DNA polymerization catalyzed by human pol γ holoenzyme has been established by using pre-steady state kinetic analysis (35, 37, 40, 41). This mechanism shows that an incoming dNTP binds to the pol γ -DNA binary complex to establish a rapid equilibrium prior to nucleotide incorporation (37, 41). Therefore, the ground state equilibrium dissociation constant of an incoming dNTP (K_d) and its maximum incorporation rate constant (k_p) can be measured by observing the nucleotide concentration dependence of the observed single-turnover rate constant (k_{obs}) (40). To examine the toxicity of gemcitabine toward human mitochondria resulting from inhibition of pol γ , we first determined the substrate specificity (k_p/K_d) of dFdCTP. Because a nucleotide analog is usually incorporated slowly, and its incorporation rate constant is comparable or smaller than the dissociation rate constant of DNA from the enzyme-DNA binary complex, the burst phase is either insignificant or does not exist. Thus, the experiments to measure the k_p/K_d value of dFdCTP were performed with pol γ in molar excess over DNA to allow the direct observation of nucleotide incorporation in a single pass of the reactants through the catalytic cycle without complications resulting from the steady state formation of products (42). In addition, because the wild-type pol γ has highly efficient 3' → 5'-exonuclease activity (41), which excises a primer from its 3' terminus and thereby complicates direct observation of the incorporation of dFdCTP, we used pol γ E200A, a well characterized single point mutant at the 3' → 5'-exonuclease active site, to determine the kinetics of dFdCTP incorporation (40). This mutant incorporates normal nucleotides with similar kinetics as the wild-type pol γ but is exonuclease-deficient (36).

To measure the pre-steady state kinetic parameters for dFdCTP incorporation, a preincubated solution of pol γ E200A (90 nM large subunit, 450 nM accessory subunit) and 5'-³²P-labeled 22/41-mer (30 nM, Table 1) was mixed and reacted with increasing concentrations of dFdCTP at 37 °C for various times. An autoradiograph gel image (Fig. 1A) showed that E200A gradually incorporated dFdCTP, as primer 22-mer was elongated to 23-mer. Each time course of product formation in Fig. 1B was fit to Equation 1 (see "Experimental Procedures") to yield an observed single-turnover rate constant, k_{obs} . The k_{obs} values were then plotted as a function of dFdCTP concentration (Fig. 1C). The data were fit to Equation 2 (see "Experimental Procedures") to yield a k_p of $2.0 \pm 0.3 \text{ s}^{-1}$ and a K_d of $21 \pm 7 \mu\text{M}$ (Table 2). The substrate specificity of dFdCTP was calculated to be $0.095 \mu\text{M}^{-1} \text{ s}^{-1}$. Similarly, we measured the k_p ($37 \pm 2 \text{ s}^{-1}$) and K_d ($0.9 \pm 0.2 \mu\text{M}$) for the incorporation of dCTP into the 22/41-mer (Table 1) under single-turnover reaction conditions (data not shown). These kinetic parameters agreed well with those that were measured under burst reaction conditions (40), thus validating our single-turnover approach. The incorporation efficiency of dCTP was then calculated to be $41 \mu\text{M}^{-1} \text{ s}^{-1}$. Thus, the discrimination, defined as the efficiency ratio of (k_p/K_d)_{dCTP}/(k_p/K_d)_{dFdCTP}, exhibited by the polymerase activity of human pol γ against dFdCTP was 432-fold (Table 2).

TABLE 1
DNA substrates

15/41-mer	5'-GGACGGCATTGGATC 3'-CCTGCCGTAACCTAGCTGCCACTCAACCAACCTGCCGACGC-5'
22/41-mer	5'-CGCAGCCGTCCAACCAACTCAC 3'-GGTCGGCAGGTTGGTTGAGTGGCAGCTAGGTTACGGCAGG-5'
23/41-mer	5'-CGCAGCCGTCCAACCAACTCAC 3'-GGTCGGCAGGTTGGTTGAGTGGCAGCTAGGTTACGGCAGG-5'
23F/41-mer ^a	5'-CGCAGCCGTCCAACCAACTCAC ^F 3'-GGTCGGCAGGTTGGTTGAGTGGCAGCTAGGTTACGGCAGG-5'
24FG/41-mer ^a	5'-CGCAGCCGTCCAACCAACTCAC ^{FG} 3'-GGTCGGCAGGTTGGTTGAGTGGCAGCTAGGTTACGGCAGG-5'
25FGT/41-mer ^a	5'-CGCAGCCGTCCAACCAACTCAC ^{FGT} 3'-GGTCGGCAGGTTGGTTGAGTGGCAGCTAGGTTACGGCAGG-5'
15/41F-mer ^a	5'-GGACGGCATTGGATC 3'-CCTGCCGTAACCTAGCTGCCACTCAACCAACCTGCCGACGC-5'
18/41F-mer ^a	5'-GGACGGCATTGGATCGAC 3'-CCTGCCGTAACCTAGCTGCCACTCAACCAACCTGCCGACGC-5'
19/41F-mer ^a	5'-GGACGGCATTGGATCGACG 3'-CCTGCCGTAACCTAGCTGCCACTCAACCAACCTGCCGACGC-5'
20/41F-mer ^a	5'-GGACGGCATTGGATCGACGG 3'-CCTGCCGTAACCTAGCTGCCACTCAACCAACCTGCCGACGC-5'
20T/41F-mer ^a	5'-GGACGGCATTGGATCGACGT 3'-CCTGCCGTAACCTAGCTGCCACTCAACCAACCTGCCGACGC-5'
21/41F-mer ^a	5'-GGACGGCATTGGATCGACGGT 3'-CCTGCCGTAACCTAGCTGCCACTCAACCAACCTGCCGACGC-5'
22/41F-mer ^a	5'-GGACGGCATTGGATCGACGGTG 3'-CCTGCCGTAACCTAGCTGCCACTCAACCAACCTGCCGACGC-5'
25/45-mer ^b	5'-GCCTCGCAGCCGTCCAACCAACTCA 3'-CGGAGCGTCGGCAGGTTGGTTGAGTGGAGCTAGGTTACGGCAGG-5'
21-19/35-mer ^c	5'-CGCAGCCGTCCAACCAACTCAC ^G TCATCCAATGCCGTCC-3' 3'-GGTCGGCAGGTTGGTTGAGTGGCAGCTAGGTTAC-5'
21F-19/35-mer ^c	5'-CGCAGCCGTCCAACCAACTCA ^F CGTCGATCCAATGCCGTCC-3' 3'-GGTCGGCAGGTTGGTTGAGTG-GCAGCTAGGTTAC-5'

^a F denotes gemcitabine.^b The template base opposite primer at the 26th base was varied to allow correct base pairing of incoming dNTP.^c The downstream strand 19-mer of substrates 21-19/35-mer and 21F-19/35-mer were 5'-phosphorylated.

Measurement of the Excision Rate Constants of Matched 3'-dFdCMP and 3'-dCMP—The 3' → 5'-exonuclease activity of human pol γ recognizes mismatched 3'-base(s) in a DNA primer and rapidly excises 1–7 mismatched bases at a rate of 1–9 nucleotides/s but slowly excises the matched 3'-terminal base of a primer (41). Although paired with template base dG, the incorporated 3'-dFdCMP in a primer may be a substrate for this 3' → 5' exonucleolytic proofreading mechanism and thereby excised. We first synthesized and purified primer 23F-mer (see “Experimental Procedures” and Table 1) and then measured the excision rate constant (k_{exo}) of 3'-dFdCMP from the DNA substrate 23F/41-mer (Table 1) by the wild-type pol γ under single-turnover reaction conditions. A preincubated solution of the wild-type pol γ (100 nM large subunit, 500 nM accessory subunit) and 75 nM 5'-[³²P]DNA (23/41-mer or 23F/41-mer) in buffer G was rapidly mixed and reacted with 2.5 mM MgCl₂ for various time intervals prior to being quenched with 0.37 M EDTA. The concentration of the remaining full-length primer *versus* reaction time was plotted and fit to Equation 3 (see “Experimental Procedures”), yielding the k_{exo} of 0.06 ± 0.02 and $0.0011 \pm 0.0001 \text{ s}^{-1}$ for the 23/41-mer and 23F/41-mer, respectively (Fig. 2 and Table 3). The k_{exo} of 23/41-mer DNA was similar to $0.05 \pm 0.01 \text{ s}^{-1}$ measured previously with a completely matched substrate 25/45-mer (Table 1) (41). Interestingly, the excision of the matched 3'-dFdCMP moiety by the wild-type pol γ was 55-fold slower than the excision of matched 3'-dCMP. This suggested that an incorporated dFdCMP likely escaped the editing process and subsequently would be embedded into the mtDNA.

Measurement of the Extension Efficiency of a Primer Terminated with 3'-dFdCMP—It is possible that an incorporated dFdCMP moiety on the 3' terminus of a DNA primer could significantly alter the ability of pol γ to extend that primer. To examine this possibility, we measured the kinetic parameters for the incorporation of correct dGTP into 23F/41-mer (Table 1) catalyzed by E200A under single-turnover conditions as described above (data not shown). dGTP was incorporated with a k_p of $1.5 \pm 0.1 \text{ s}^{-1}$, a K_d of $7.2 \pm 0.9 \mu\text{M}$, and a k_p/K_d of $0.21 \mu\text{M}^{-1} \text{ s}^{-1}$ (Table 2). In comparison, a matched dGTP is incorporated into normal 25/45-mer (Table 1) with a k_p of $37 \pm 2 \text{ s}^{-1}$ and a K_d of $0.8 \pm 0.1 \mu\text{M}$, which defined a k_p/K_d of $45 \mu\text{M}^{-1} \text{ s}^{-1}$ (40). Thus, the 3'-dFdCMP decreased the incorporation efficiency of the first downstream nucleotide by 214-fold, suggesting that an incorporated gemcitabine was problematic for primer extension. Such an inhibitory effect may persist beyond 1 nucleotide. Therefore, to examine if an embedded gemcitabine inhibited the incorporation of the second downstream nucleotide, we prepared primer 24FG-mer (see “Experimental Procedures”). We then measured the kinetic parameters of correct dTTP incorporation into 24FG/41-mer (Table 1) catalyzed by E200A (data not shown). Under single-turnover reaction conditions as described above, dTTP was incorporated with a k_p of $2.8 \pm 0.1 \text{ s}^{-1}$, a K_d of $0.5 \pm 0.1 \mu\text{M}$, and a k_p/K_d of $5.6 \mu\text{M}^{-1} \text{ s}^{-1}$ (Table 2). In comparison, given a canonical DNA substrate of 25/45-mer (Table 1), correct dTTP is incorporated with a k_p of 25 s^{-1} , a K_d of $0.6 \mu\text{M}$, and a k_p/K_d of $39 \mu\text{M}^{-1} \text{ s}^{-1}$ (Table 4) (40). Thus, primer 3'-dFdCMP lowered the second downstream nucleotide incorporation efficiency by 7-fold. Interestingly, the third nucleotide (dCTP) downstream from

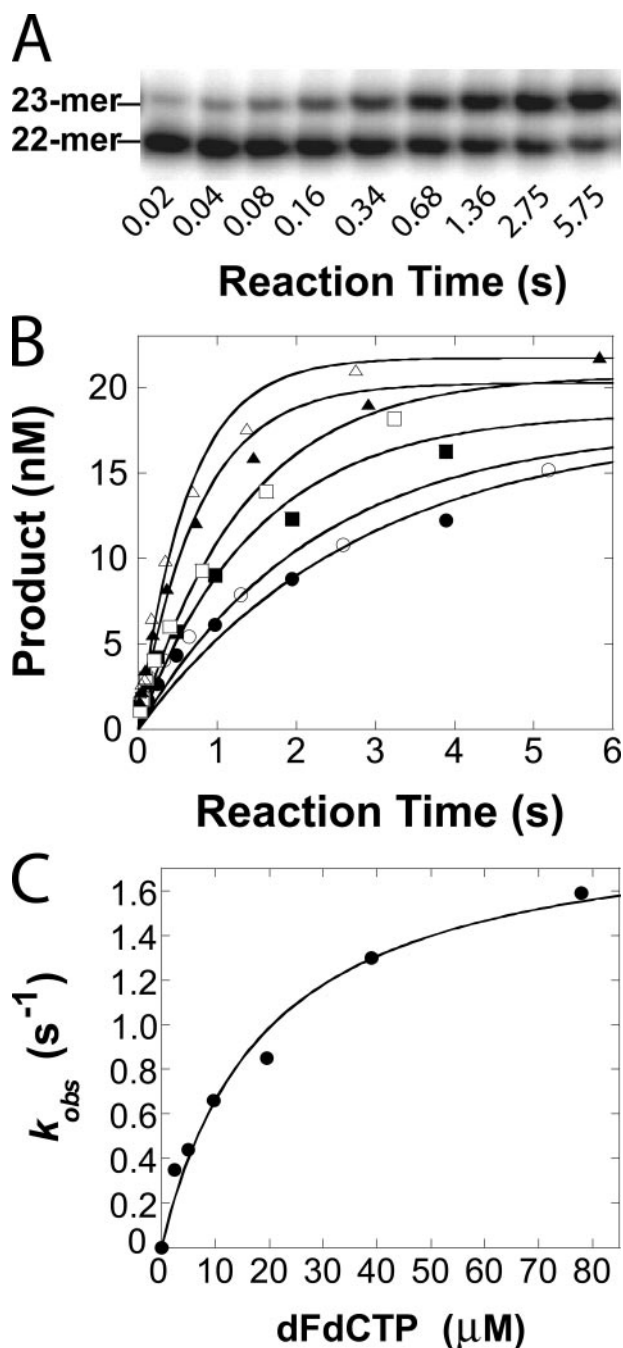


FIGURE 1. Concentration dependence of observed single-turnover rate constant of dFdCTP incorporation. *A*, autoradiograph gel image shows the incorporation of dFdCTP (16 μM) catalyzed by a pol γ mutant E200A. *B*, preincubated solution of E200A (90 nM), pol γ accessory subunit (450 nM), and 5'- ^{32}P -labeled 22/41-mer (30 nM) was rapidly mixed with increasing concentrations of dFdCTP-Mg $^{2+}$ (2.4 μM , \bullet ; 4.9 μM , \circ ; 9.7 μM , \blacksquare ; 19.5 μM , \square ; 39 μM , \blacktriangle ; 78 μM , \triangle) and reacted at 37 $^{\circ}\text{C}$ for increasing times. The *solid lines* were fit to Equation 1 using nonlinear regression which determined the observed rate constants, k_{obs} . *C*, k_{obs} values were plotted as a function of dFdCTP concentration. The data (\bullet) were fit to Equation 2 using nonlinear regression, thus yielding a k_p of $2.0 \pm 0.3 \text{ s}^{-1}$ and a K_d of $21 \pm 7 \mu\text{M}$.

the embedded dFdCMP was incorporated into 25FGT/41-mer with similar efficiency as it was incorporated into normal 22/41-mer (data not shown). Therefore, an incorporated dFdCMP in the DNA primer only affected two downstream nucleotide incorporation events, especially the first one. However, it did not terminate primer elongation.

TABLE 2

Kinetic parameters of single nucleotide incorporation catalyzed by pol γ E200A under single-turnover conditions at 37 $^{\circ}\text{C}$

DNA	dNTP	K_d	k_p	k_p/K_d	Efficiency ratio ^a
		μM	s^{-1}	$\mu\text{M}^{-1} \text{s}^{-1}$	
22/41-mer	dCTP	0.9 ± 0.2	37 ± 2	41	1
22/41-mer	dFdCTP	21 ± 7	2.0 ± 0.3	0.095	432
23F/41-mer	dGTP	7.2 ± 0.9	1.5 ± 0.1	0.21	214 ^b
24FG/41-mer	dTTP	0.5 ± 0.1	2.8 ± 0.1	5.6	7 ^b
25/45-mer	FlAUTP ^c	2.9 ± 0.7^c	24 ± 2^c	8.3 ^c	5

^a Data are calculated as $(k_p/K_d)_{\text{correct dNTP into normal DNA}}$

$(k_p/K_d)_{\text{correct dNTP into DNA containing dFdCMP}}$

^b $(k_p/K_d)_{\text{correct dNTP into normal DNA}}$ is from Ref. 40.

^c Data are from Ref. 40.

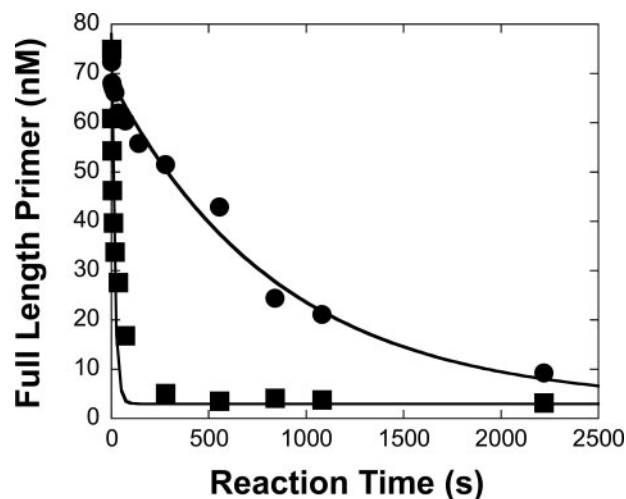


FIGURE 2. Measurement of the rate constant of DNA primer degradation by the 3' \rightarrow 5' exonuclease proofreading activity of the wild-type pol γ . A preincubated solution of the wild-type pol γ (100 nM), pol γ accessory subunit (500 nM), and 23/41-mer or 23F/41-mer (75 nM) in buffer G was rapidly mixed with 2.5 mM MgCl $_2$ and reacted for various time intervals. The excision reaction was quenched by the addition of 0.37 M EDTA. The concentration of the remaining full-length primer *versus* time was plotted and fit to Equation 3 (23/41-mer, \blacksquare ; 23F/41-mer, \bullet) yielding a k_{exo} of $0.06 \pm 0.02 \text{ s}^{-1}$ for 23/41-mer and $0.0011 \pm 0.0001 \text{ s}^{-1}$ for 23F/41-mer.

TABLE 3

Excision rate constants for the 3' \rightarrow 5' exonuclease activity of the wild-type human pol γ holoenzyme under single-turnover conditions at 37 $^{\circ}\text{C}$

DNA	Fast phase	Fast phase	Slow phase	Slow phase
	$k_{\text{exo},1}$	amplitude	$k_{\text{exo},2}$	amplitude
	s^{-1}	%	s^{-1}	%
23/41-mer	0.06 ± 0.02	NA ^a	NA	NA
23F/41-mer	0.0011 ± 0.0001	NA	NA	NA
20/41F-mer	0.028 ± 0.006	NA	NA	NA
20T/41F-mer	0.2 ± 0.2	17 ± 8	0.008 ± 0.002	83 ± 8

^a NA means not applicable.

Running Start Primer Extension Assays—To investigate whether or not a dFdC lesion embedded in a DNA template affects DNA synthesis catalyzed by human pol γ , we first synthesized template 41F-mer (Table 1) as described under "Experimental Procedures." To examine the nucleotide incorporation profile, a running start primer elongation assay was performed to evaluate the ability of the wild-type pol γ (90 nM) to bypass the template dFdCMP lesion in 15/41F-mer (30 nM, Table 1) in the presence of four dNTPs (100 μM each). In comparison, a similar running start assay was also performed with an undamaged control substrate

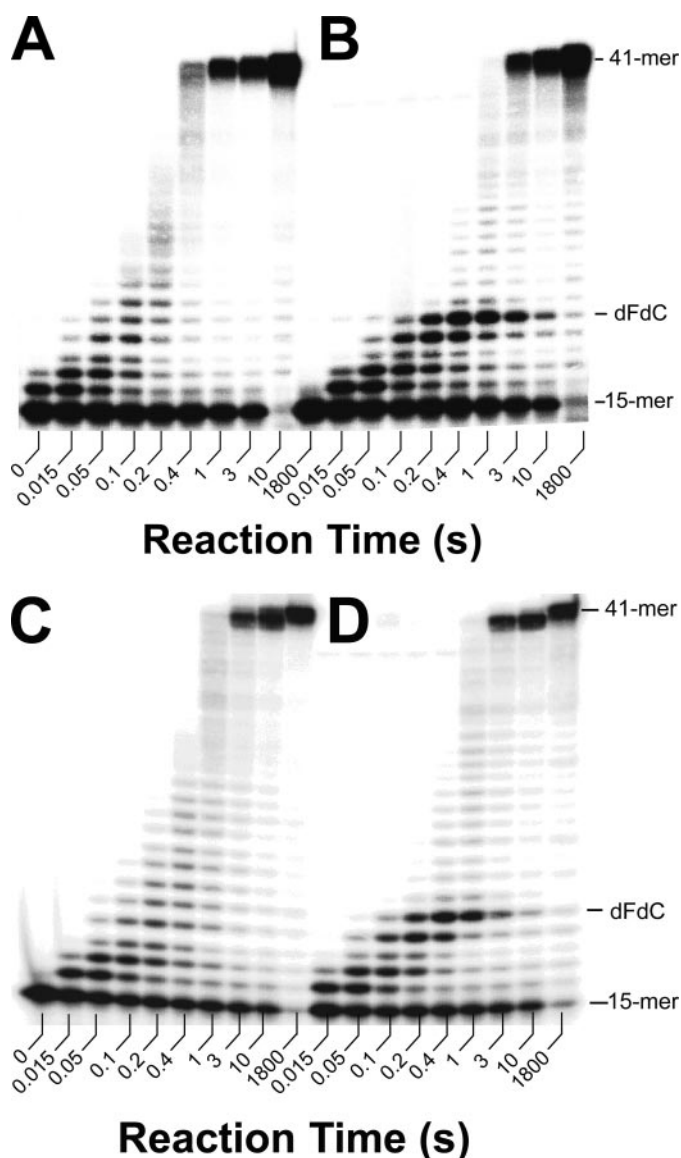


FIGURE 3. Running start primer elongation catalyzed by the wild-type pol γ and the exonuclease-deficient mutant E200A. A solution of control substrate 15/41-mer (A and C, 30 nM each) or DNA substrate 15/41F-mer (B and D, 30 nM each), preincubated with the wild-type pol γ (A and B, 90 nM) or E200A (C and D, 90 nM) and pol γ accessory subunit (450 nM) in buffer G, was rapidly mixed with 2.5 mM MgCl₂ and 100 μ M each of dATP, dCTP, dGTP, and dTTP. Reactions were allowed to continue for various time intervals before being quenched by the addition of 0.37 M EDTA. Product lengths and the position of the embedded dFdC moiety in the template are indicated.

15/41-mer (30 nM, Table 1). With the 15/41-mer, the wild-type pol γ holoenzyme was able to extend the 15-mer primer to the full-length 41-mer in 1 s (Fig. 3A). This rate was consistent with the average maximum rate constant (38 s^{-1}) of single nucleotide incorporation into normal 25/45-mer (Table 4) (40). In contrast, the wild-type pol γ paused opposite the dFdCMP lesion and 1 base downstream of the dFdCMP lesion in the 15/41F-mer (Fig. 3B). Consequently, the full-length product 41-mer was formed in 3 s, rather than just 1 s as observed with control 15/41-mer (Fig. 3A). Although the synthesis of the 41-mer was delayed, Fig. 3B showed that the wild-type pol γ eventually bypassed the dFdCMP lesion.

TABLE 4

Kinetic parameters of single nucleotide incorporation into DNA containing a template base dFdCMP catalyzed by pol γ E200A under single-turnover conditions at 37 $^{\circ}$ C

DNA	dNTP	K_d	k_p	k_p/K_d	Efficiency ratio ^a
		μM	s^{-1}	$\mu\text{M}^{-1}\text{s}^{-1}$	
18/41F-mer	dGTP	1.1 ± 0.2	2.1 ± 0.1	1.9	2.4×10^1
19/41F-mer	dGTP	150 ± 10	6.3 ± 0.2	0.042	1.1×10^3
20/41F-mer	dTTP	6.0 ± 0.5	0.11 ± 0.01	0.018	2.2×10^3
21/41F-mer	dGTP	5 ± 2	1.7 ± 0.4	0.34	1.3×10^2
22/41F-mer	dATP	0.7 ± 0.1	8.3 ± 0.3	12	4.8
25/45-mer ^b	dATP	0.8 ± 0.1	45 ± 1	57	
25/45-mer ^b	dTTP	0.6 ± 0.2	25 ± 2	39	
25/45-mer ^b	dGTP	0.8 ± 0.1	37 ± 2	45	
25/45-mer ^b	dCTP	0.9 ± 0.2	43 ± 2	47	

^a Data are calculated as $(k_p/K_d)_{\text{correct}}$ dNTP into 25/45-mer¹

^b $(k_p/K_d)_{\text{dNTP}}$ into DNA containing a template base dFdCMP.

^c Kinetic parameters are from Ref. 40.

To examine whether or not the 3' \rightarrow 5'-exonuclease activity of human pol γ plays any role in the bypass of the dFdCMP lesion, we performed the same running start primer elongation assays with pol γ E200A. Fig. 3, C and D, showed that the product formation patterns with both 15/41-mer and 15/41F-mer were almost identical to the patterns in Fig. 3, A and B, respectively. Thus, the 3' \rightarrow 5'-exonuclease activity appeared not to recognize template base dFdC as a lesion and was dispensable for its bypass.

Measurement of the Excision Rate Constant of Primer 3'-dNMP Opposite Template Base dFdCMP—To quantitatively interrogate the effect of an embedded dFdCMP moiety on the 3' \rightarrow 5'-exonuclease activity of pol γ , we synthesized two DNA substrates (see "Experimental Procedures") as follows: 20/41F-mer and 20T/41F-mer (Table 1) which contain a 3'-terminal "correct" base pair and a mismatch, respectively. Under single-turnover conditions, the wild-type pol γ holoenzyme was found to excise the primer 3'-bases of the 20/41F-mer with a k_{exo} of $0.028 \pm 0.006 \text{ s}^{-1}$ (Table 3). This k_{exo} value was roughly 2-fold slower than the k_{exo} of $0.06 \pm 0.02 \text{ s}^{-1}$ observed with a normal substrate 23/41-mer (Table 3). In comparison, the time course of the cleavage of the 20T/41F-mer by the wild-type pol γ under single-turnover reaction conditions was biphasic and fit to Equation 4 (see "Experimental Procedures") to yield a $k_{\text{exo},1}$ of $0.2 \pm 0.2 \text{ s}^{-1}$ and an amplitude of $(17 \pm 8)\%$ in the fast phase and a $k_{\text{exo},2}$ of $0.008 \pm 0.002 \text{ s}^{-1}$ and an amplitude of $(83 \pm 8)\%$ in the slow phase (data not shown). Similar biphasic kinetics are also observed previously with the cleavage of normal DNA containing a single 3'-mismatched base but with larger k_{exo} values in the fast phase (1.1 s^{-1}) and slow phase (0.04 s^{-1}) (40). These data confirmed that template base dFdC inhibited the proofreading activity of human pol γ .

Measurement of Incorporation Efficiency of Nucleotides Opposite Template dFdCMP—The reason that pol γ strongly paused in Fig. 3, B and D, is likely because the dFdCMP lesion altered the local template structure and significantly decreased the incorporation efficiencies of adjacent nucleotides. To evaluate this hypothesis, we measured the incorporation efficiencies of correct nucleotides into 18/41F-mer, 19/41F-mer, 20/41F-mer, 21/41F-mer, and 22/41F-mer (Table 1) catalyzed by pol γ E200A under single-turnover reaction conditions (data not shown). The measured kinetic parameters in Table 4 indi-

TABLE 5
Fidelity at the two strong pause sites

DNA	dNTP	K_d	k_p	k_p/K_d	Fidelity ^a
		μM	s^{-1}	$\mu\text{M}^{-1} \text{s}^{-1}$	
19/41F-mer	dGTP	150 \pm 10	6.3 \pm 0.2	4.2 \times 10 ⁻²	1
19/41F-mer	dTTP ^b	110 \pm 30	0.0015 \pm 0.0002	1.4 \times 10 ⁻⁵	3.0 \times 10 ³
20/41F-mer	dTTP	6.0 \pm 0.5	0.11 \pm 0.01	1.8 \times 10 ⁻²	1
20/41F-mer	dATP ^b	120 \pm 20	0.0059 \pm 0.0003	4.9 \times 10 ⁻⁵	3.7 \times 10 ²

^a Data are calculated as $(k_p/K_d)_{\text{correct dNTP}}/(k_p/K_d)_{\text{incorrect dNTP}}$.^b Boldface type indicates incorrect nucleotide.

cated that, relative to the corresponding values with normal 25/45-mer (Table 1) (40), the ground-state binding affinity ($1/K_d$) of a correct incoming nucleotide was up to 2 orders of magnitude lower at the two strong pause sites but was within 5-fold at the non-pause sites. In comparison, the maximum nucleotide incorporation rate constant dropped by 3 orders of magnitude at the second strong pause site, whereas the k_p values at other positions were 5–30-fold lower than the corresponding parameters given for 25/45-mer (Table 4). As expected, the substrate specificity (k_p/K_d) values were more informative in demonstrating why pol γ paused at the two positions in Fig. 3, B and D. Before encountering the template base dFdCMP, pol γ E200A incorporated correct dGTP into 18/41F-mer with only 24-fold lower substrate specificity compared with normal 25/45-mer (Table 4). The efficiency ratio increased from 2.4×10^{-1} to 1.1×10^3 when pol γ E200A incorporated dGTP opposite dFdCMP and to 2.2×10^3 when pol γ E200A incorporated dTTP into 20/41F-mer to extend the primer and bypass dFdCMP. These significant decreases in the efficiency ratio indicated that pol γ was inefficient at incorporating nucleotides at these two positions and paused (Fig. 3, B and D). After pol γ bypassed the dFdCMP, the efficiency ratios for the next two downstream nucleotide incorporations (Table 4) decreased to 130 and 4.8, respectively. Although we did not measure the substrate specificity of dGTP incorporation into 23/41F-mer, we expect the inhibitory effect of an embedded gemcitabine in the template will disappear at this position and further downstream. Notably, based on the low nucleotide incorporation efficiency with 21/41F-mer (Table 4), pol γ E200A was expected to pause at this position. However, the pause was not obvious in Fig. 3D. This discrepancy was because the k_p of 1.7 s^{-1} is relatively fast, and the reaction times were relatively long.

Measurement of Nucleotide Incorporation Fidelity at the Pause Sites—Opposite dFdCMP, pol γ may favor mismatched dNTPs over dGTP. To examine this possibility, each dNTP (200 μM) was reacted individually with a preincubated solution of E200A and 19/41F-mer (Table 1) for 15 s or 1 h. The supplemental Fig. 3A showed that pol γ E200A preferred to incorporate dGTP opposite dFdCMP at both time intervals. Interestingly, dTTP was misincorporated multiple times. This suggested that pol γ E200A may have a high tendency to misincorporate dTTP. To check if this was the case, we measured the k_p/K_d value for dTTP incorporation into 19/41F-mer under single-turnover conditions (data not shown). The calculated fidelity in Table 5 indicated that pol γ E200A only favored dGTP over dTTP by 3,000-fold, which was much lower than the 6.4×10^5 -fold observed with normal 25/45-mer (43). Thus, the

fidelity of nucleotide incorporation opposite dFdCMP was lowered by 213-fold.

To further examine the effect of template lesion dFdCMP on polymerase fidelity, we tested whether or not pol γ was error-prone when extending primer 20-mer to 21-mer. Opposite template base dAMP, pol γ E200A incorporated correct dTTP more efficiently than incorrect nucleotides (supplemental Fig. 3B), and dATP was the most favored incorrect nucleotide. We further measured the kinetic parameters of dATP misincorporation into 20/41F-mer under single-turnover conditions (data not shown). pol γ E200A favored correct dTTP over incorrect dATP by only 370-fold (Table 5), which was 757-fold lower than the corresponding fidelity (2.8×10^5) observed with canonical 25/45-mer (43).

DISCUSSION

Konerding *et al.* (44) have solved the solution-phase structure of an Okazaki fragment (12-bp) with an internally embedded dFdCMP using NMR. This structure reveals the following perturbations caused by gemcitabine: (i) the ribose ring of the dFdCMP moiety forms a 3'-*endo* pucker as opposed to the canonical 2'-*endo* pucker of a dCMP moiety; (ii) the highly electronegative geminal difluoro group increases the electron density in its vicinity; and (iii) the two fluorine atoms in dFdCMP are physically larger than the corresponding hydrogen atoms in dCMP. These factors are predicted to affect DNA polymerization catalyzed by DNA polymerases, including human pol γ holoenzyme.

Inhibition of DNA Synthesis by Gemcitabine as an Incoming Nucleotide—The pre-steady state kinetic data in Table 2 revealed that relative to dCTP, dFdCTP was incorporated into normal 22/41-mer by pol γ with an 18.5-fold lower k_p , whereas the K_d was 23-fold higher, leading to a 432-fold lower k_p/K_d value. These kinetic differences can be rationalized as follows. (i) Although dFdCTP is not the same as embedded dFdCMP in DNA, we assume that dFdCTP initially adopts the 3'-*endo* pucker once it is bound to form the ground-state ternary complex (E-DNA-dNTP). (ii) In order for the phosphodiester bond formation to occur, the conformation of the bound dFdCTP has to be converted to the canonical 2'-*endo* pucker to allow proper alignment of the primer 3'-OH and the α -phosphate of dFdCTP. (iii) The energy penalty for this conformational conversion should reduce the incorporation rate of dFdCTP. Moreover, the electron-withdrawing difluoro group withdraws electron density from the triphosphate of dFdCTP and thereby reduces the reactivity of the α -phosphate moiety during phosphodiester bond formation. This difluoro group also increases the size of dFdCTP, which may cause a steric clash with the polymerase active site residues. Relative to dCTP, the altered conformation, electrostatics, and physical size likely weakened the interactions between dFdCTP, the template base dGMP, and polymerase active site residues, hence the lower binding affinity of dFdCTP.

Although the efficiency ratio in Table 2 defined dFdCTP as a 432-fold less efficient substrate than dCTP, the incorporation probability of dFdCTP relative to dCTP *in vivo*, theoretically defined as $\{[dFdCTP]/[dCTP]\} \times \{(k_p/K_d)_{dFdCTP}/(k_p/K_d)_{dCTP}\}$, is likely to be high. Self-potential activities of gemcitabine

Gemcitabine Inhibits Human DNA Polymerase γ

(supplemental Fig. 2) (28, 29) are known to bring about a dramatic cytoplasmic accumulation of dFdCTP, thereby raising the cellular concentration ratio of [dFdCTP]/[dCTP]. For example, Heine-mann *et al.* (26) found that mammalian cells exposed to 100 μM gemcitabine for 4 h showed that cellular pools of dCTP were reduced by 50% and that the cytoplasmic concentration of dFdCTP had risen to over 1 mM. Because relative sizes of individual dNTP pools in the cytosol and mitochondria are similar (45), we expect to find an enriched dFdCTP pool in mitochondria as well. Therefore, it is reasonable to assume that incorporation of dFdCMP into mitochondrial DNA *in vivo* may be significant.

Compared with FIAUTP, another non-chain-terminating nucleoside analog, dFdCTP is incorporated by pol γ with a 7-fold higher K_d value and a 12-fold slower k_p value (Table 2). Comparison of the efficiency ratios for these two nucleotide analogs indicated that dFdCTP is an 86-fold less efficient substrate for human mitochondrial DNA polymerase, which corresponds to and may account for the diminished toxicity of gemcitabine compared with the highly toxic FIAU.

Following dFdCTP incorporation, the DNA primer terminated with 3'-dFdCMP is likely to adopt the 3'-*endo* pucker conformation as observed in the solution structures of gemcitabine embedded in DNA (44). The electron density of its 3'-OH group should be lowered by the electron-withdrawing fluorine group, thereby rendering the 3'-OH group less nucleophilic. These factors are expected to lower the suitability of the dFdCMP-terminated DNA primer as a substrate for pol γ and hinder the incorporation of the next incoming nucleoside triphosphate. This hypothesis was supported by the observation that correct dGTP was incorporated into 23F/41-mer (Table 1) with a 25-fold smaller k_p and a 214-fold lower catalytic efficiency compared with the canonical DNA template 25/45-mer (Table 2) (40). However, the inhibitory effect of a 3'-terminated dFdCMP primer on the catalytic efficiency of extension via correct dNTP incorporation was reduced by 7-fold for the second downstream nucleotide incorporation (Table 2) and was not observed for the third and subsequent nucleotide incorporations (data not shown). Interestingly, human DNA polymerases α and ϵ , which belong to the B-family, have also been found to inefficiently incorporate dFdCTP. However, in contrast to what has been observed for the A-family enzyme pol γ , these B-family human DNA polymerases exhibit masked chain termination following dFdCMP incorporation. For example, Huang *et al.* (22) demonstrate that, following the incorporation of a 3' dFdCMP moiety on a DNA primer, DNA elongation is possible but is very strongly inhibited. In a time period of 1,800 s, only a portion of the primer was extended past the masked termination event, and of those elongation events, only a few dNTPs were added. In contrast, pol γ did not exhibit the expected masked chain termination and was able to extend a DNA primer containing 3'-dFdCMP although with decreased nucleotide incorporation efficiency at the first two downstream positions (Table 2). So far, there are no reported studies on how human DNA polymerases α and ϵ bypass a template lesion dFdCMP. Interestingly, Fig. 3 showed that within 3 s pol γ was highly successful at bypassing the dFdCMP lesion, albeit in an error-prone manner (Table 4). For wild-type pol γ , only 4% less full-length product was produced in the 3-s time period given a

template with embedded dFdCMP (Fig. 3B) compared with the control template (Fig. 3A) (22). Additionally, DNA polymerase θ , the only other member of the A-family DNA polymerases yet identified in humans, has been shown to bypass abasic site and thymine glycol DNA lesions but is completely unable to bypass a variety of DNA lesions resulting from exposure to UV light and cisplatin-based chemotherapy drugs (46). However, the ability of pol θ to bypass dFdCMP or any other nucleoside analog within the context of DNA has yet to be examined.

Incorporated dFdCMP Eludes Editing Mechanism—Upon incorporation at the 3' DNA primer terminus, the 3' \rightarrow 5'-exonuclease activity of pol γ may recognize and excise incorporated dFdCMP as a lesion because of its different conformation and electrostatic character compared with dCMP. Surprisingly, Table 3 revealed that the excision rate of dFdCMP from the DNA primer 3' terminus (0.0011 s^{-1}) was 55-fold slower than the excision of a corresponding primer terminated with 3'-dCMP (control substrate 23/41-mer). At a nucleotide concentration of 100 μM , pol γ E200A incorporated dGTP into 23F/41-mer with a k_p of 1.5 s^{-1} (Table 2). Based on the principle of kinetic partitioning, the probability of the exonuclease function editing dFdGMP, $(k_{\text{exo}}/(k_{\text{exo}} + k_p)) \times 100 = (0.0011/(0.0011 + 1.5)) \times 100$, is calculated to be 0.07%. This probability is much lower than the 80% observed for the correction of a mismatched canonical dNMP (41). Taken together, although the extension of a dFdCMP-terminated primer is 25-fold slower than the extension of a canonical DNA primer, the reduced excision rate constant and thus the extremely low probability of exonuclease editing activity by pol γ increase the likelihood of an incorporated dFdCMP persisting and becoming embedded within the mitochondrial genome if it is not removed by other DNA repair mechanisms. Furthermore, given that mtDNA repair is limited and inefficient (47), persistence of dFdCMP within mtDNA is predicted to be likely. Finally, the toxic side effects of chain-terminating nucleoside analog drugs recede when therapy with the drugs is discontinued (36). However, in the case of FIAU, which has a free 3'-OH group and is not a chain-terminating nucleoside analog, toxicity has been shown to persist and worsen despite immediate withdrawal of the drug, eventually leading to the death of five patients from severe mitochondrial toxicity (48). This suggests that the mitochondria may be able to effectively remove chain-terminating nucleoside analogs and resume normal mtDNA replication, but nucleoside analogs that do not chain terminate, and therefore can become part of the mitochondrial genome, may exert long term toxicity.

Inhibition of Human pol γ -catalyzed DNA Synthesis by Gemcitabine as a Template Base—Fig. 3, B and D, showed that human pol γ holoenzyme, both wild-type and E200A, paused strongly opposite the template base dFdCMP and at the next template position. The kinetic data in Table 4 demonstrated that the efficiency ratio correlated well with the observed pause patterns (Fig. 3). The efficiency ratio (2.2×10^3) reached the poorest value when pol γ attempted to extend the 20/41F-mer, the strongest pause site (Fig. 3, B and D). The second strongest pause site, where pol γ attempted to incorporate dGTP opposite dFdCMP, correlated with the second poorest efficiency ratio value of 1.1×10^3 (Table 4). Our analysis also revealed

that, in comparison with the extension of canonical 25/45-mer DNA template, nucleotide incorporation efficiency of pol γ dropped to between 5- and 132-fold at 1 nucleotide preceding dFdCMP and at 2–3 nucleotides downstream of the dFdCMP lesion (Table 4). However, Fig. 3, *B* and *D*, did not show obvious pausing by pol γ at these positions. This lack of pausing was because of the relatively high k_p values ($2-8\text{ s}^{-1}$) and long reaction times that allowed pol γ to rapidly elongate the corresponding intermediate products. Taken together, one embedded dFdCMP moiety in a DNA template unfavorably affected five nucleotide incorporation events surrounding that lesion. This inhibitory effect may also be due to local DNA structural perturbations caused by dFdCMP (44) as described above. The 3'-endo pucker conformation of template base dFdCMP likely caused unproductive base pairing between an incoming dGTP and dFdCMP, leading to a 188-fold higher K_d value for the binding of dGTP to pol γ 19/41F-mer (Table 4). Similarly, dFdCMP also decreased the binding affinity of the next 2 downstream nucleotides by 6–10-fold before recovering to normal. The predicted decrease in the structural integrity of the DNA duplex caused by the presence of a dFdCMP moiety with a 3'-endo pucker is supported by the fact that the melting temperature of the 12-bp Okazaki fragment is lowered by 4.3 °C in the presence of an internal dFdCMP (44). Such a noncanonical conformation of dFdCMP in a template should also affect the positioning of an incoming dNTP for in-line attack by the primer's 3'-OH group during phosphodiester bond formation. If this indeed is occurring, it would readily explain the reduction in k_p values observed. The negative impact was largest (227-fold) for dTTP incorporation into 20/41F-mer. Interestingly, the inhibitory effect of gemcitabine was larger as a template base than as an incoming nucleotide when we compared the efficiency ratios in Tables 2 and 4. This suggested that if a ribose pucker conversion is necessary for correct orientation of the nucleotide triphosphate prior to the chemistry step, it may be more difficult when gemcitabine is constrained within the template sequence than when it is either an incoming nucleotide triphosphate or a 3'-primer terminal base. However, the reason for these interesting observations cannot be unambiguously determined here.

Unfaithful Bypass of Template dFdCMP—When a template lesion causes a DNA polymerase to pause, the enzyme tends to catalyze 5' \rightarrow 3' DNA polymerization in an error-prone manner. This general trend was found to hold true when pol γ bypassed the template dFdCMP moiety. Table 5 shows that the polymerase activity of pol γ has a fidelity of 3.7×10^2 to 3.0×10^3 at the two strong pause sites (Fig. 3, *B* and *D*), which is significantly lower than the corresponding fidelity of 2.8×10^5 to 6.4×10^5 determined with canonical DNA substrate 25/45-mer (43). Thus, pol γ was 200–800-fold less faithful upon encountering a dFdCMP template lesion, thus promoting DNA mutagenesis. To compound these mutagenic events, the misincorporated canonical nucleotide (for example 3'-dTTP in 20T/41F-mer) was excised more slowly than a single 3'-mismatched primer base in a canonical DNA template (40). In addition, the matched primer terminal 3'-dGMP in 20/41F-mer was removed at half the speed of another correctly paired, canonical 3'-primer terminal dNMP (23/41-mer substrate, Table 3).

Therefore, the inhibited exonuclease activity as a result of the template-embedded dFdCMP may actually facilitate nucleotide misincorporation by slowing the 3' \rightarrow 5'-exonuclease activity of pol γ . With respect to the editing function of pol γ , the currently established mechanism is that the primer 3'-mismatched base is transferred from the polymerase active site to the 3' \rightarrow 5'-exonuclease active site for excision, whereas the template strand remains at the polymerase active site of pol γ (41). With this in mind, there arise at least two possible explanations for the observed exonucleolytic rate. Either the presence of dFdCMP in the template directly inhibited the exonucleolytic activity or it hindered the transfer of the 3'-primer terminus to the proofreading active site or possibly both. More studies in our laboratory are under way to examine these possibilities.

Potential Relevance to Observed Gemcitabine Clinical Toxicity—Our kinetic analysis directly confirmed that gemcitabine, as both an incoming nucleotide and as a template base, inhibited DNA synthesis catalyzed by human pol γ . Moreover, our studies also revealed that each template dFdCMP was a mutagenic “hot spot” during DNA replication. Additionally, mutagenic effects may be exerted by gemcitabine metabolites within the mitochondria. For instance, it is known that gemcitabine metabolites cause cellular dNTP pool imbalances by inhibiting ribonucleotide reductase (23, 24), CTP synthetase (25, 26), and dCMP deaminase (27). Therefore, gemcitabine therapy is also likely to cause an imbalance of mitochondrial nucleotide pools. Such imbalances have been found previously to be mutagenic to the mitochondrial genome (49) and lead to disease states such as mitochondrial neurogastrointestinal encephalomyopathy (50). Considering that mammalian cells have 1,000–5,000 copies of the mitochondrial genome (51, 52) and given that mtDNA replication occurs continuously throughout the entire cell cycle (45, 53), these inhibitory and mutagenic effects of gemcitabine may result in growing mitochondrial genomic instability over time and, like FIAU, may be persistent.

Acknowledgments—We acknowledge the contributions of both Harold Lee and Chris Hamilton for preparing human DNA polymerase γ .

REFERENCES

- Crino, L., Scagliotti, G. V., Ricci, S., De Marinis, F., Rinaldi, M., Gridelli, C., Ceribelli, A., Bianco, R., Marangolo, M., Di Costanzo, F., Sassi, M., Barni, S., Ravaioli, A., Adamo, V., Portalone, L., Cruciani, G., Masotti, A., Ferrara, G., Gozzelino, F., and Tonato, M. (1999) *J. Clin. Oncol.* **17**, 3522–3530
- Burris, H. A., III, Moore, M. J., Andersen, J., Green, M. R., Rothenberg, M. L., Modiano, M. R., Cripps, M. C., Portenoy, R. K., Storniolo, A. M., Tarassoff, P., Nelson, R., Dorr, F. A., Stephens, C. D., and Von Hoff, D. D. (1997) *J. Clin. Oncol.* **15**, 2403–2413
- Morandi, P. (2006) *Ann. Oncol.* **17**, Suppl. 5, V177–V180
- Lorusso, D., Di Stefano, A., Fanfani, F., and Scambia, G. (2006) *Ann. Oncol.* **17**, Suppl. 5, V188–V194
- Sallah, S., Wan, J. Y., and Nguyen, N. P. (2001) *Br. J. Haematol.* **113**, 185–187
- Einhorn, L. H., Stender, M. J., and Williams, S. D. (1999) *J. Clin. Oncol.* **17**, 509–511
- Kubicka, S., Rudolph, K. L., Tietze, M. K., Lorenz, M., and Manns, M. (2001) *Hepatogastroenterology* **48**, 783–789
- Catimel, G., Vermorken, J. B., Clavel, M., de Mulder, P., Judson, I., Sessa,

- C., Piccart, M., Brunsch, U., Verweij, J., Wanders, J., Franklin, H., Kaye, S. B., and the EORTC Early Clinical Trials Group (1994) *Ann. Oncol.* **5**, 543–547
9. Mutch, D. G., and Bloss, J. D. (2003) *Gynecol. Oncol.* **90**, S8–S15
 10. Dumontet, C., Morschhauser, F., Solal-Celigny, P., Bouafia, F., Bourgeois, E., Thieblemont, C., Leleu, X., Hequet, O., Salles, G., and Coiffier, B. (2001) *Br. J. Haematol.* **113**, 772–778
 11. Dalbagni, G., Russo, P., Bochner, B., Ben-Porat, L., Sheinfeld, J., Sogani, P., Donat, M. S., Herr, H. W., and Bajorin, D. (2006) *J. Clin. Oncol.* **24**, 2729–2734
 12. Fracasso, P. M., Tan, B. R., Jr., Grieff, M., Stephenson, J., Jr., Liapis, H., Umbeck, N. L., Von Hoff, D. D., and Rowinsky, E. K. (1999) *J. Natl. Cancer Inst.* **91**, 1779–1780
 13. Pfisterer, J., Plante, M., Vergote, I., du Bois, A., Hirte, H., Lacave, A. J., Wagner, U., Stahle, A., Stuart, G., Kimmig, R., Olbricht, S., Le, T., Emerich, J., Kuhn, W., Bentley, J., Jackisch, C., Luck, H. J., Rochon, J., Zimmermann, A. H., and Eisenhauer, E. (2006) *J. Clin. Oncol.* **24**, 4699–4707
 14. Airoidi, M., Cattel, L., Passera, R., Pedani, F., Milla, P., and Zanon, C. (2006) *Pancreas* **32**, 44–50
 15. Shirai, T., Hirose, T., Noda, M., Ando, K., Ishida, H., Hosaka, T., Ozawa, T., Okuda, K., Ohnishi, T., Ohmori, T., Horichi, N., and Adachi, M. (2006) *Lung Cancer* **52**, 181–187
 16. Mackey, J. R., Mani, R. S., Selner, M., Mowles, D., Young, J. D., Belt, J. A., Crawford, C. R., and Cass, C. E. (1998) *Cancer Res.* **58**, 4349–4357
 17. Mackey, J. R., Yao, S. Y., Smith, K. M., Karpinski, E., Baldwin, S. A., Cass, C. E., and Young, J. D. (1999) *J. Natl. Cancer Inst.* **91**, 1876–1881
 18. Marce, S., Molina-Arcas, M., Villamor, N., Casado, F. J., Campo, E., Pastor-Anglada, M., and Colomer, D. (2006) *Haematologica* **91**, 895–902
 19. Blackstock, A. W., Lightfoot, H., Case, L. D., Tepper, J. E., Mukherji, S. K., Mitchell, B. S., Swarts, S. G., and Hess, S. M. (2001) *Clin. Cancer Res.* **7**, 3263–3268
 20. Richardson, K. A., Vega, T. P., Richardson, F. C., Moore, C. L., Rohloff, J. C., Tomkinson, B., Bendele, R. A., and Kuchta, R. D. (2004) *Biochem. Pharmacol.* **68**, 2337–2346
 21. Ruiz van Haperen, V. W., Veerman, G., Vermorken, J. B., and Peters, G. J. (1993) *Biochem. Pharmacol.* **46**, 762–766
 22. Huang, P., Chubb, S., Hertel, L. W., Grindey, G. B., and Plunkett, W. (1991) *Cancer Res.* **51**, 6110–6117
 23. Shao, J., Zhou, B., Chu, B., and Yen, Y. (2006) *Curr. Cancer Drug Targets* **6**, 409–431
 24. Plunkett, W., Huang, P., Searcy, C. E., and Gandhi, V. (1996) *Semin. Oncol.* **23**, 3–15
 25. Davidson, J. D., Ma, L., Flagella, M., Geeganage, S., Gelbert, L. M., and Slapak, C. A. (2004) *Cancer Res.* **64**, 3761–3766
 26. Heinemann, V., Schulz, L., Issels, R. D., and Plunkett, W. (1995) *Semin. Oncol.* **22**, 11–18
 27. Neff, T., and Blau, C. A. (1996) *Exp. Hematol.* **24**, 1340–1346
 28. Plunkett, W., Huang, P., Xu, Y. Z., Heinemann, V., Grunewald, R., and Gandhi, V. (1995) *Semin. Oncol.* **22**, 3–10
 29. Heinemann, V., Xu, Y. Z., Chubb, S., Sen, A., Hertel, L. W., Grindey, G. B., and Plunkett, W. (1992) *Cancer Res.* **52**, 533–539
 30. Verstappen, C. C., Postma, T. J., Hoekman, K., and Heimans, J. J. (2003) *J. Neurooncol.* **63**, 201–205
 31. Dormann, A. J., Grunewald, T., Wigglinghaus, B., and Huchzermeyer, H. (1998) *Lancet* **351**, 644
 32. Lewis, W., and Dalakas, M. C. (1995) *Nat. Med.* **1**, 417–422
 33. Semino-Mora, C., Leon-Monzon, M., and Dalakas, M. C. (1997) *Lab. Invest.* **76**, 487–495
 34. Brahams, D. (1994) *Lancet* **343**, 1494–1495
 35. Johnson, A. A., Tsai, Y., Graves, S. W., and Johnson, K. A. (2000) *Biochemistry* **39**, 1702–1708
 36. Johnson, A. A., Ray, A. S., Hanes, J., Suo, Z., Colacino, J. M., Anderson, K. S., and Johnson, K. A. (2001) *J. Biol. Chem.* **276**, 40847–40857
 37. Graves, S. W., Johnson, A. A., and Johnson, K. A. (1998) *Biochemistry* **37**, 6050–6058
 38. Roettger, M. P., Fiala, K. A., Sompalli, S., Dong, Y., and Suo, Z. (2004) *Biochemistry* **43**, 13827–13838
 39. Fiala, K. A., Duym, W. W., Zhang, J., and Suo, Z. (2006) *J. Biol. Chem.* **281**, 19038–19044
 40. Johnson, A. A., and Johnson, K. A. (2001) *J. Biol. Chem.* **276**, 38090–38096
 41. Johnson, A. A., and Johnson, K. A. (2001) *J. Biol. Chem.* **276**, 38097–38107
 42. Johnson, K. A. (1992) *Enzymes* **20**, 1–61
 43. Lee, H. R., and Johnson, K. A. (2006) *J. Biol. Chem.* **281**, 36236–36240
 44. Konerding, D., James, T. L., Trump, E., Soto, A. M., Marky, L. A., and Gmeiner, W. H. (2002) *Biochemistry* **41**, 839–846
 45. Ferraro, P., Nicolosi, L., Bernardi, P., Reichard, P., and Bianchi, V. (2006) *Proc. Natl. Acad. Sci. U. S. A.* **103**, 18586–18591
 46. Ukai, A., Maruyama, T., Mochizuki, S., Ouchida, R., Masuda, K., Kawamura, K., Tagawa, M., Kinoshita, K., Sakamoto, A., Tokuhisa, T., and O-Wang, J. (2006) *Genes Cells* **11**, 111–121
 47. Bogenhagen, D. F. (1999) *Am. J. Hum. Genet.* **64**, 1276–1281
 48. McKenzie, R., Fried, M. W., Sallie, R., Conjeevaram, H., Di Bisceglie, A. M., Park, Y., Savarese, B., Kleiner, D., Tsokos, M., Luciano, C., Pruett, T., Stotka, J. L., Straus, S. E., and Hoofnagle, J. H. (1995) *N. Engl. J. Med.* **333**, 1099–1105
 49. Song, S., Wheeler, L. J., and Mathews, C. K. (2003) *J. Biol. Chem.* **278**, 43893–43896
 50. Nishino, I., Spinazzola, A., and Hirano, M. (1999) *Science* **283**, 689–692
 51. Bogenhagen, D., and Clayton, D. A. (1974) *J. Biol. Chem.* **249**, 7991–7995
 52. Shmookler Reis, R. J., and Goldstein, S. (1983) *J. Biol. Chem.* **258**, 9078–9085
 53. Bogenhagen, D., and Clayton, D. A. (1977) *Cell* **11**, 719–727